J. Soc. Cosmet. Chem., 45, 21–33 (January/February 1994)

The protective effect of a broad-spectrum sunscreen against chronic UVA radiation in hairless mice: A histologic and ultrastructural assessment

LORRAINE H. KLIGMAN and PEISHU ZHENG, *Department of Dermatology, University of Pennsylvania School of Medicine, Philadelphia, PA 19104-6142.*

Received July 12, 1993.

Synopsis

Long-wavelength UVA (>340 nm) has been shown capable of inducing dermal damage with chronic exposure. This study assesses the effect of a broad spectrum (SPF-15) sunscreen containing avobenzone (Parsol 1789) in comparison to an oxybenzone-containing sunscreen. Albino hairless mice were irradiated thrice weekly (100 J/cm^2/exposure) for a cumulative dose of 8000 J/cm^2 after 32 weeks. Sunscreens were applied (2 μl/cm^2) to two groups of mice. The third group was unprotected, and a fourth served as a normal unirradiated control.

Unprotected, irradiated mice developed epidermal acanthosis and dermal elastic fiber hyperplasia with increased glycosaminoglycans. Mice protected with the avobenzone-containing sunscreen had marginal epidermal hyperplasia but no other histologic damage. By contrast, mice protected with the oxybenzone-containing sunscreen, surprisingly, had damage that exceeded what was seen in unprotected mice. Electron microscopy confirmed the histologic findings and revealed further ultrastructural differences between the treatment groups. The unexpected exacerbation of photodamage with the oxybenzone-containing sunscreen was very likely not due to the oxybenzone but rather to irritation induced by some component in the vehicle. All SPF-15 sunscreens, by definition, must protect against sunburn. The consequences of chronic exposure may be quite different and are clinically relevant.

INTRODUCTION

As a result of recent studies with hairless mice, the evidence is accumulating that chronic exposure to either full-spectrum (>320 nm) or long-wavelength UVA (UVA I: >340 nm) induces dermal connective tissue damage (1–7). With histochemical (1–5), ultrastructural (6), and biochemical techniques (5,7), elastic fiber hyperplasia, increases in the glycosaminoglycans (GAGs) of the ground substance, and a change in the susceptibility of collagen to enzymatic digestion have been described. Reports on sunscreen protection against these UVA-induced changes are beginning to appear. Broad-spectrum, oxybenzone-containing sunscreens (peak absorption: ~320 nm) (8) of sun protection factor (SPF) 15 have been shown histologically to prevent the elastic fiber hyperplasia and the increases in GAGs induced by solar-simulating radiation that in-

cludes a large UVA component (1). An SPF-15 oxybenzone-containing sunscreen was tested in hairless mice by Bissett *et al.* (3) using a low-irradiance black light UVA lamp (peak emission ~355 nm). These workers report no protection by this sunscreen against UVA-induced skin changes such as sagging and increased GAGs. However, avobenzone (Parsol 1789: 4-tert. butyl -4′-methoxydibenzoylmethane: peak absorption ~360 nm) in a 7% solution in carbitol resulted in retardation of UVA-induced skin sagging, thickening, and amelioration of histological alterations. Harrison *et al.* (9) examined a 0.75% concentration of avobenzone in an oil-and-water emulsion in hairless mice irradiated with sub-erythemal doses of UVA as emitted by unfiltered Philips TL 10 tubes (peak emission ~360 nm). Unlike Bissett *et al.* (3), they found no protection against histologic dermal damage. This may be due, among other factors, to the low concentration of avobenzone and the small, but energetically significant, emission by these tubes of UVB at 302 and 313 nm.

Broad-spectrum sunscreens have not been examined by using pure UVA with an emission spectrum that closely approximates solar UVA for efficacy against photoaging changes. Thus, there is still some question regarding their efficacy against UVA I (>340 nm). We decided to use the hairless mouse to compare the protective effect of two commercially available broad-spectrum sunscreens against chronic exposure to this portion of the UVA waveband. Both sunscreens had an SPF of 15, with one containing avobenzone as the UVA absorber, and the other, oxybenzone.

MATERIALS AND METHODS

ANIMALS AND TREATMENT GROUPS

There were four groups of 12 Skh-hairless-1 female albino mice, ages 6–8 weeks (Temple University Health Sciences Center, Philadelphia, PA). They were housed individually under General Electric F40 GO gold fluorescent tubes, which emit no UV radiation (12-hour on/off cycle). Treatment groups were as follows: 1) UVA only; 2) UVA with avobenzone-containing (3%) commercial sunscreen (SS-A); 3) UVA with oxybenzone-containing (3%) commercial sunscreen (SS-B) SPF-15*; and 4) unirradiated, untreated controls. Sunscreens were applied to the entire dorsal surface of the mice (2 $\mu l/cm^2$) five minutes prior to each exposure.

Vehicles for the sunscreens were not deemed necessary at the start of the experiment, nor were they available to us. The results with SS-B were totally unexpected.

RADIATION SOURCE AND EXPOSURE SCHEDULE

The high-intensity UVASUN 3000 lamp provided UVA I radiation (340–400 nm). At mouse level, a distance of 65 cm from the lamp, irradiance was ~15 mW/cm^2 as measured with an IL 700 A research radiometer (International Light, Inc., Newburyport, MA). The UVA sensor has peak sensitivity at ~360 nm. The emission spectrum of this lamp has been published previously (2). To ensure that no radiation below 340

* The formulation tested is no longer commercially available.

nm was transmitted, new filters were installed at the beginning of the experiment and again after 400 hours of use. Spectroradiometric readings of our lamp have shown that lower wavelengths begin to appear at 500 hours (unpublished results). Ambient temperature at the level of the mice was kept at ~27°C by two small fans. An erythemic dose in naive animals with this UVA source is 50–60 J/cm^2. The exposures of 100 J/cm^2 were therefore reached gradually by 25 J/cm^2 increments over the first two weeks, to avoid erythema in the unprotected mice. With a thrice weekly exposure (M, W, F) for ~32 weeks, the total cumulative dose was 8000 J/cm^2.

MICROSCOPY

On the Monday following the final Friday exposure, dorsal skin biopsies (2 × ½ cm) were taken and processed for light microscopy. The histochemical stains were hematoxylin and eosin (H & E) for general histology, Luna's aldehyde fuchsin for elastic fibers (10), Van Gieson's for collagen, and Mowry's colloidal iron for GAGs. Slides were evaluated in a coded manner. Adjacent dorsal skin was also processed for electron microscopy.

ULTRASTRUCTURE

Specimens were fixed in Karnovsky's solution, followed by 1% osmium tetroxide, and were embedded in Epon 812. Ultrathin sections (70 nm) were stained with a tannic acid-uranyl acetate solution (11) followed by Reynold's lead citrate, each for 10 minutes. These were examined in a Hitachi model H700 electron microscope.

COLLAGEN FIBER MEASUREMENTS

Collagen fiber diameters were measured on 3–5 electron micrographs per treatment group at 42,500× magnification. Two to three squares measuring 5 × 5 cm were drawn on each micrograph in areas where fibers were clearly in cross section. All fibers within the squares were measured.

RESULTS

CLINICAL APPEARANCE

At the end of the 32-week irradiation period, unprotected UVA-exposed mice had the thickened, yellowed, sagging skin typically induced by this waveband (3). The skin of most SS-A–protected mice was only slightly thickened and pale, but was not distinctly yellow. A few of the mice retained the pinkish skin of unirradiated controls. SS-B–protected mice developed some scaling less than halfway through the experiment. This was judged to be irritation due to the sunscreen. By the end of the irradiation period, more than half of the animals had thickened leathery patches on the central dorsum (Figure 1).

Two mice in the unprotected group had a total of three 2-mm papillomas. In the SS-B group, one mouse had one 2-mm papilloma. There were no tumors in the unirradiated or SS-A groups.

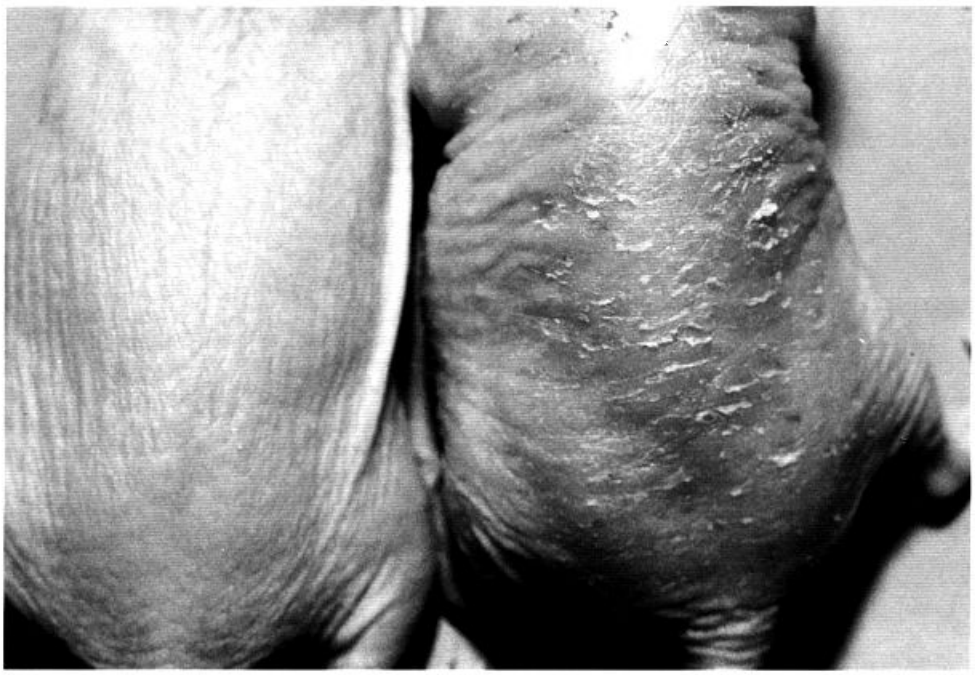

Figure 1. UVA-irradiated mice (32 weeks: 8,000 J/cm^2). Skin of SS-A–protected animal (left) has normal-appearing, pale pink skin. SS-B–treated animal (right) is scaling and leathery, with pin-point erosions (×2).

HISTOLOGY

General (H&E). Unirradiated hairless mice (age ~40 weeks) have a thin 3–4-cell-layer epidermis. The collagen is mainly concentrated in the upper dermis, whereas the lower dermis contains mainly a single row of keratinizing cysts, typical for this mouse, along with a variable amount of lipocytes (1).

After 8000 J/cm^2 of long-wavelength UVA, the unprotected skin was more than twice as thick, with an acanthotic epidermis of ~7 cell layers. There was mild cellular disorder and a few foci of parakeratosis, but very little atypia. Enlarged dermal cysts proliferated up to three rows (Figure 2A).

Skin protected with SS-A was mainly unthickened (Figure 2B). The epidermis was slightly acanthotic (~5 cell layers) but was without loss of order, atypia, or parakeratosis. Dermal cysts, while usually in a single row, were occasionally in two rows. This is within the normal range of variability for these mice.

Skin protected with SS-B appeared as damaged as UVA-irradiated, unprotected skin. Epidermal atypia was more pronounced, and inflammatory infiltrates were present in the dermis and epidermis (Figure 2C). Cyst proliferation was more variable than in UVA only.

Elastic fibers. The elastic fibers in unirradiated mice are thin and very sparse (12). After UVA irradiation, most specimens showed mild elastic fiber hyperplasia and a few foci of moderate hyperplasia. Fibers were also slightly thickened and tortuous (Figure 3A). With SS-A protection, the elastic fibers were as thin and sparse as in unirradiated skin

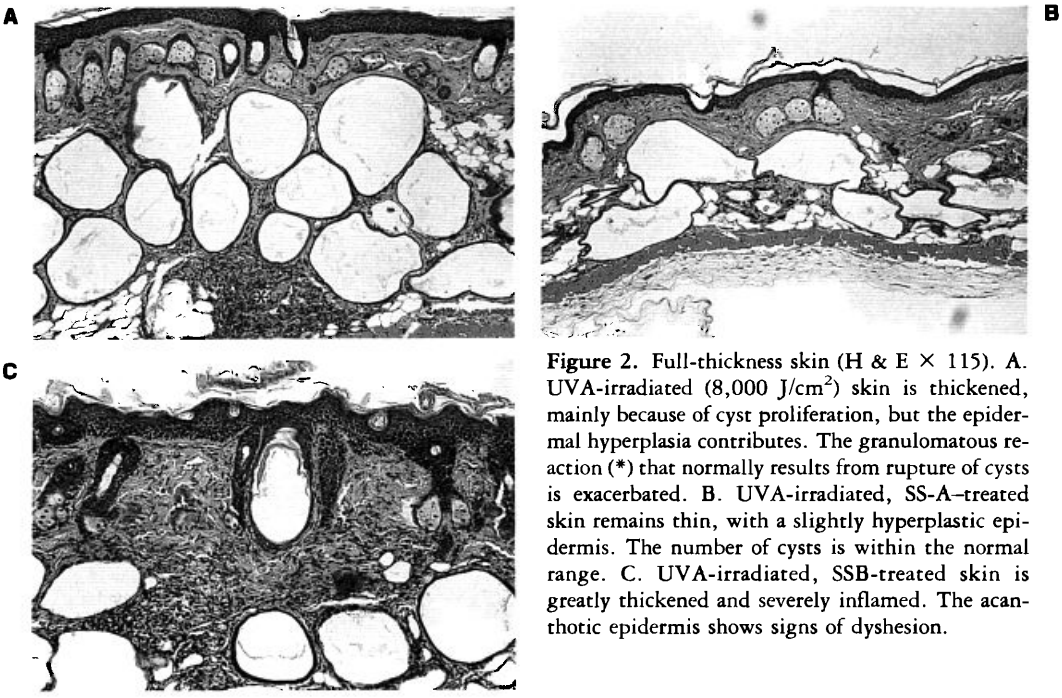

Figure 2. Full-thickness skin (H & E × 115). A. UVA-irradiated (8,000 J/cm^2) skin is thickened, mainly because of cyst proliferation, but the epidermal hyperplasia contributes. The granulomatous reaction (*) that normally results from rupture of cysts is exacerbated. B. UVA-irradiated, SS-A–treated skin remains thin, with a slightly hyperplastic epidermis. The number of cysts is within the normal range. C. UVA-irradiated, SSB-treated skin is greatly thickened and severely inflamed. The acanthotic epidermis shows signs of dyshesion.

(Figure 3B). Specimens from the SS-B group had a degree of elastic fiber hyperplasia that was more severe than in unprotected, irradiated skin (Figure 3C). In areas of severe inflammation, elastotic clumps were beginning to form.

Collagen. Normal collagen stains a bright crimson with Van Gieson's stain. Confirming earlier studies (1,2), chronic UVA irradiation did not alter the staining properties. Normal staining was also maintained in SS-A–protected skin (Figure 3D). In the SS-B specimens, there were occasional foci with reduced staining (Figure 3E), an indication of alteration to the collagen.

Glycosaminoglycans. Normal hairless mouse skin contains minute amounts of the blue-staining material identified as GAGs by histochemistry (12). After UVA irradiation, dermal GAGs were increased, and the normally red-staining collagen had a blue tone, as if coated with GAGs. Intercellular epidermal GAGs were also increased (Figure 3F). SS-A–protected skin appeared similar to unirradiated skin (Figure 3G). To the contrary, SS-B specimens showed varying degrees of increased GAGs, ranging from a few foci to many. Epidermal GAGs were increased in all SS-B specimens (Figure 3H).

ULTRASTRUCTURE

Epidermis. In normal, unirradiated skin, basal epidermal cells are closely adherent to one another. Chronic UVA radiation induced gaps between the cells that SS-A prevented (Figures 4A & B). The basement membrane at the dermal-epidermal junction was not duplicated in either case.

Collagen. Unlike with UVB (6), collagen fibers in cross section retained sharp outlines after chronic UVA exposure. The diameter of fibers in normal skin is diverse, with a

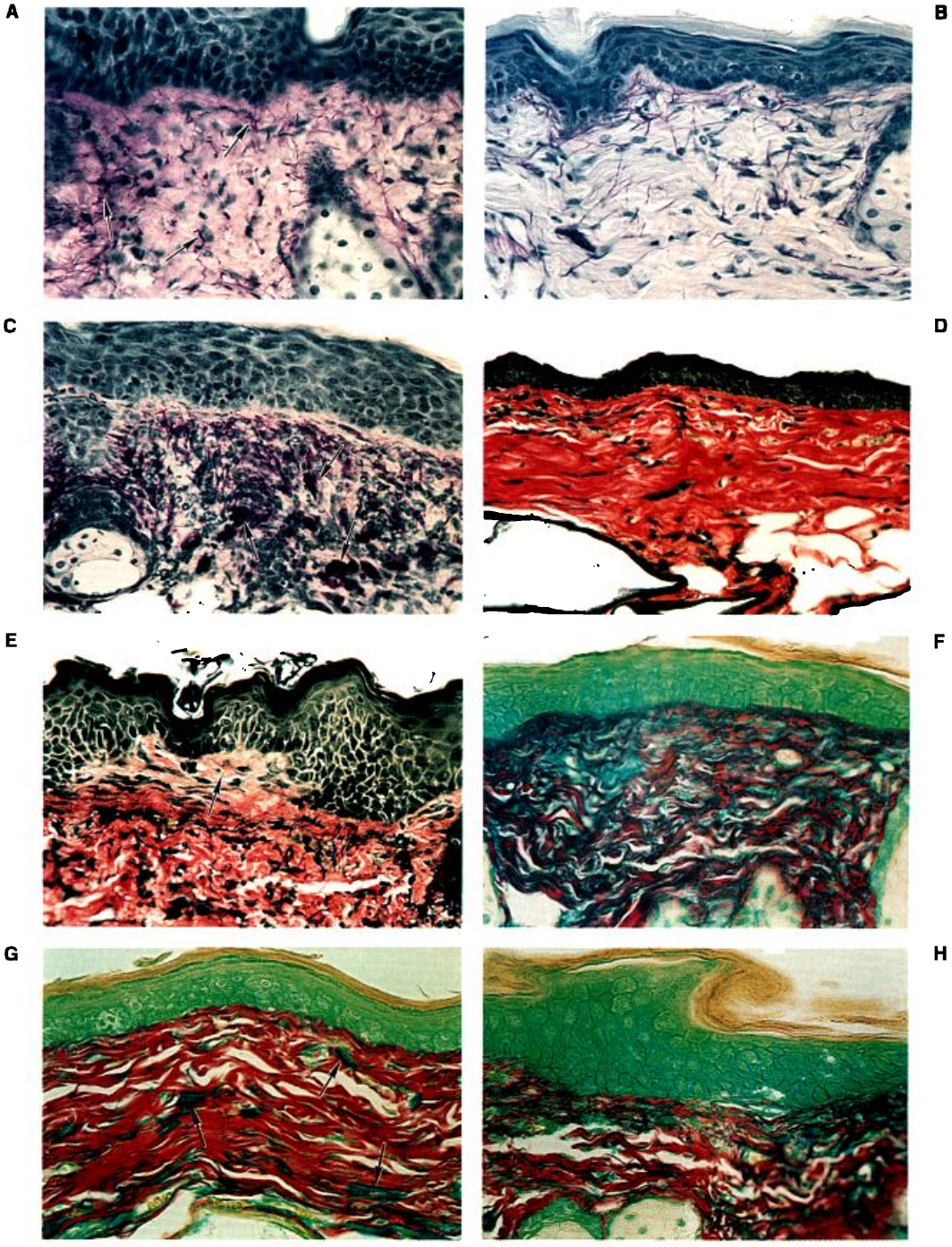
A
B
C
D
E
F
G
H

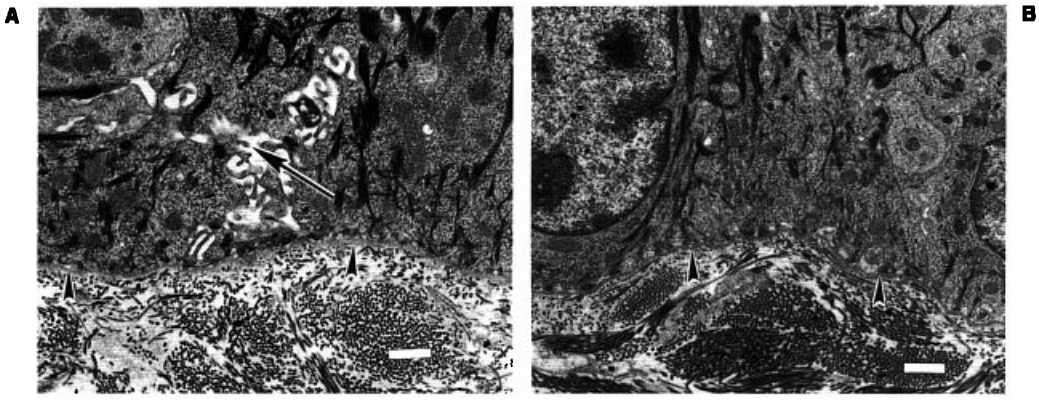

Figure 4. Epidermis. A. UVA radiation-induced extensive gap formation between basal cells (→). The basement membrane was not duplicated (▶). Magnification ×7,800. Bar = 1 μm. B. Protection with SS-A prevented gap formation, and the basement membrane remained unduplicated (▶). Magnification ×7,800. Bar = 1 μm.

range of 45–245 nm and the vast majority (80%) measuring 90–140 nm. UVA rendered it less variable, with a shift to smaller diameters (45–150 nm) and with 80% measuring 70–120 nm. SS-A protection preserved a more normal range (45–220 nm), with 80% measuring the same as in normal skin. With SS-B, diameter measurements were more similar to those with UVA alone (Figure 5).

Elastic Fibers. Normally, elastic fibers are very sparsely distributed in the upper dermis. The microfibrillar component is visible to varying degrees, depending on the amount of elastin matrix. This can be partial or almost complete, with microfibrils visible only at the periphery (11). Chronic UVA radiation induced elastic fiber hyperplasia. The fibers often appeared to aggregate into longer fibers heavily coated with elastin (Figure 6A). Other fibers had a range of matrix deposition that was similar to that in normal skin. UVA also induced the production of disorganized masses of microfibrils with little or no elastin coating (Figure 6A, inset). With SS-A protection, elastic fiber hyperplasia was greatly reduced (Figure 6B). The excess deposition of the randomly arrayed microfibrils was prevented. Microfibrils appeared mainly in organized fashion, as in a fiber, coated with the normal varying amounts of elastin (Figure 6B), inset).

Figure 3. Connective tissue histology. A, B, C. Elastic fibers (Luna's stain ×460). A. UVA irradiated (8,000 J/cm^2)—A mild hyperplasia (→) and twisting of the fibers is accompanied by an abnormal purple-pink staining of the dermal matrix. B. UVA irradiated, SS-A treated—Elastic fiber content is within the normal range, fibers are not tortuous, and the dermal matrix has the normal pale-lavender color. C. UVA irradiated, SS-B treated—Severe elastic fiber hyperplasia intermingled with an inflammatory infiltrate and mast cells (→). D, E. Collagen (Van Gieson's stain ×370): D. UVA irradiated SS-A treated—As in normal and unprotected UVA irradiated skin, collagen stains a uniform crimson color. E. UVA irradiated, SS-B treated—A small area with reduced affinity for the stain (→). The dyshesive epidermis is clearly seen. F–H. Glycosaminoglycans (Mowry's stain ×460): F. UVA irradiated—The blue-staining dermal and intercellular epidermal GAGs are greatly increased. G. UVA irradiated, SS-A treated—Dermal GAGs are extremely sparse, as in unirradiated skin. The major blue-staining structures are mast cells (→). Intercellular epidermal GAGs are marginally increased. H. UVA irradiated, SS-B treated—Dermal GAGs are moderately increased, and the intercellular epidermal GAGs are striking.

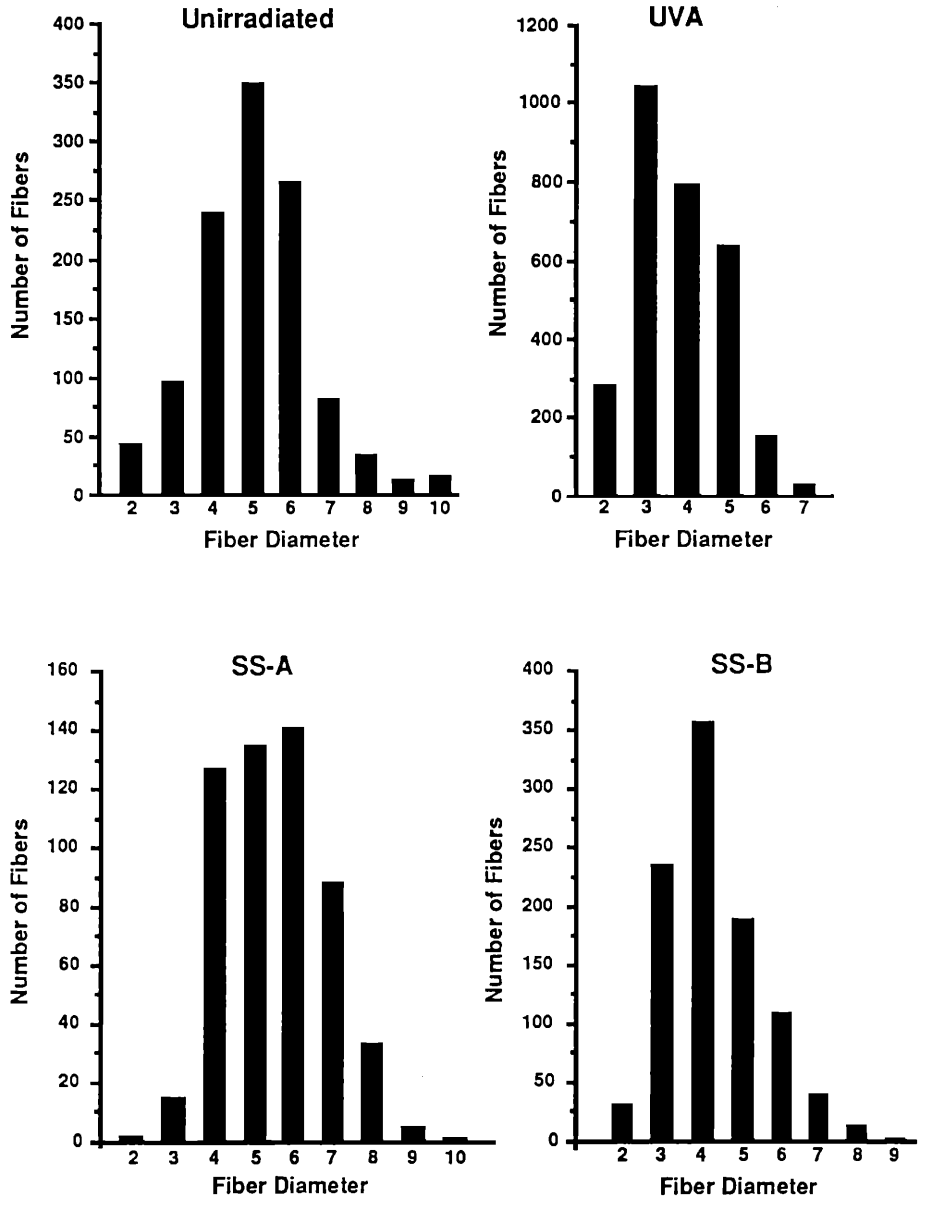

Figure 5. Collagen fiber diameter. Unirradiated skin had a broad range of diameters, with the majority measuring 4–6 mm at ×42,500 magnification. UVA-irradiated skin had a more narrow size range, with most fibers measuring 3–5 mm at ×42,500 magnification. With SS-A protection, fiber diameters were similar to those in unirradiated skin, whereas with SS-B, fiber diameters resembled those in unprotected, UVA-irradiated skin.

VASCULATURE

The cutaneous vasculature appeared to be extremely sensitive to UVA-induced injury. The basement membrane surrounding most vessels was greatly duplicated, up to 14 layers, compared to the normal 3–5 (Figure 7A). In addition, endothelial cells showed

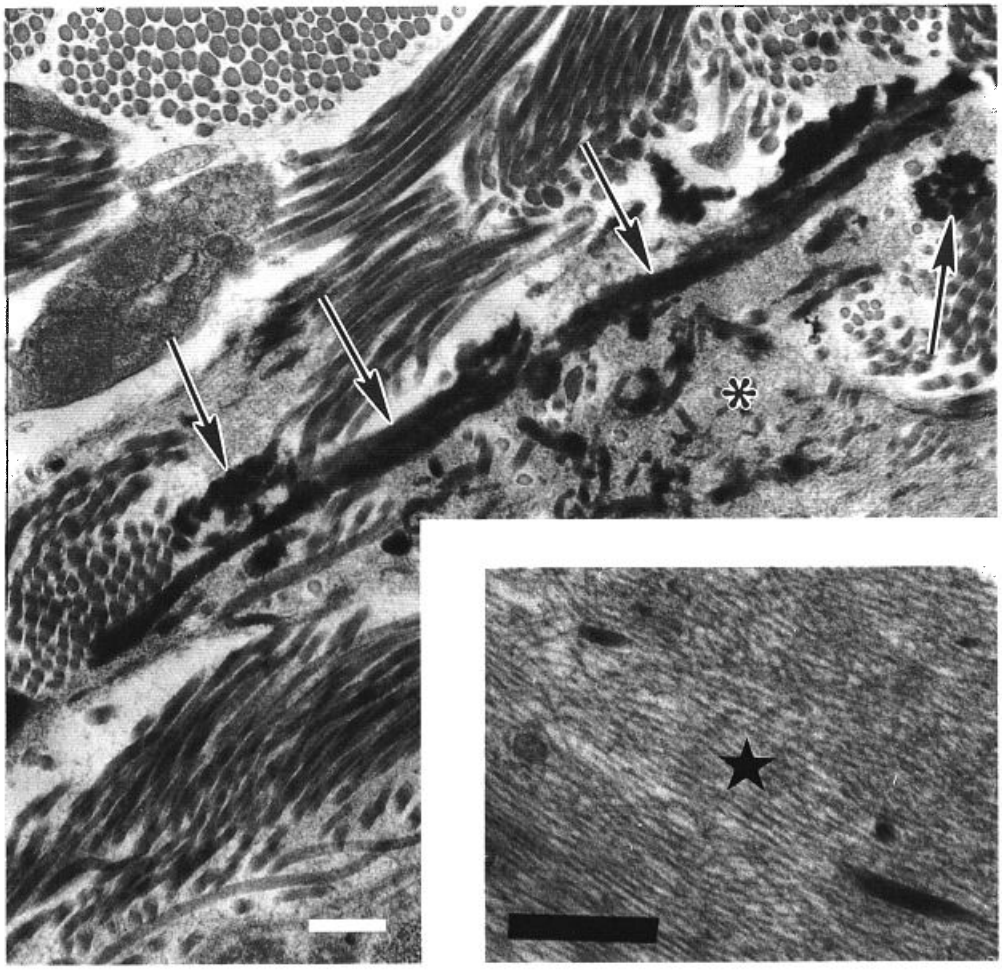

Figure 6. Elastic fibers. A. UVA radiation produced elastic fiber hyperplasia in mouse skin, which normally contains sparse elastic tissue. Many fibers were elongated and densely coated with black-staining elastin matrix (→). Masses of microfibrils (*) lacking elastin coating were present. Magnification ×20,800. Bar = .05 μm. Inset: Uncoated microfibrils (★) at higher magnification. Magnification ×37,500. Bar = .05 μm.

signs of severe damage, including extensive vesiculation of the cytoplasm, areas of extreme thinning, gaps, and mitochondrial swelling with rupture of cristae. Mitochondria in various other cell types were similarly affected. Virtually all of the UVA-induced injury was prevented by SS-A (Figure 7B). An occasional endothelial cell showed some thinning or mild vesiculation of the cytoplasm, but this was within the range of normal findings.

SS-B. Confirming histologic findings, SS-B failed to protect against UVA-induced damage. Elastic fibers were hyperplastic, microfibril deposition was increased, vascular basement membranes were greatly duplicated, and endothelial cells showed the typical UVA-induced damage. These will be described in a subsequent publication. Notably, unlike with either UVA alone or with SS-A protection, inflammatory cells were abundant (Figure 8).

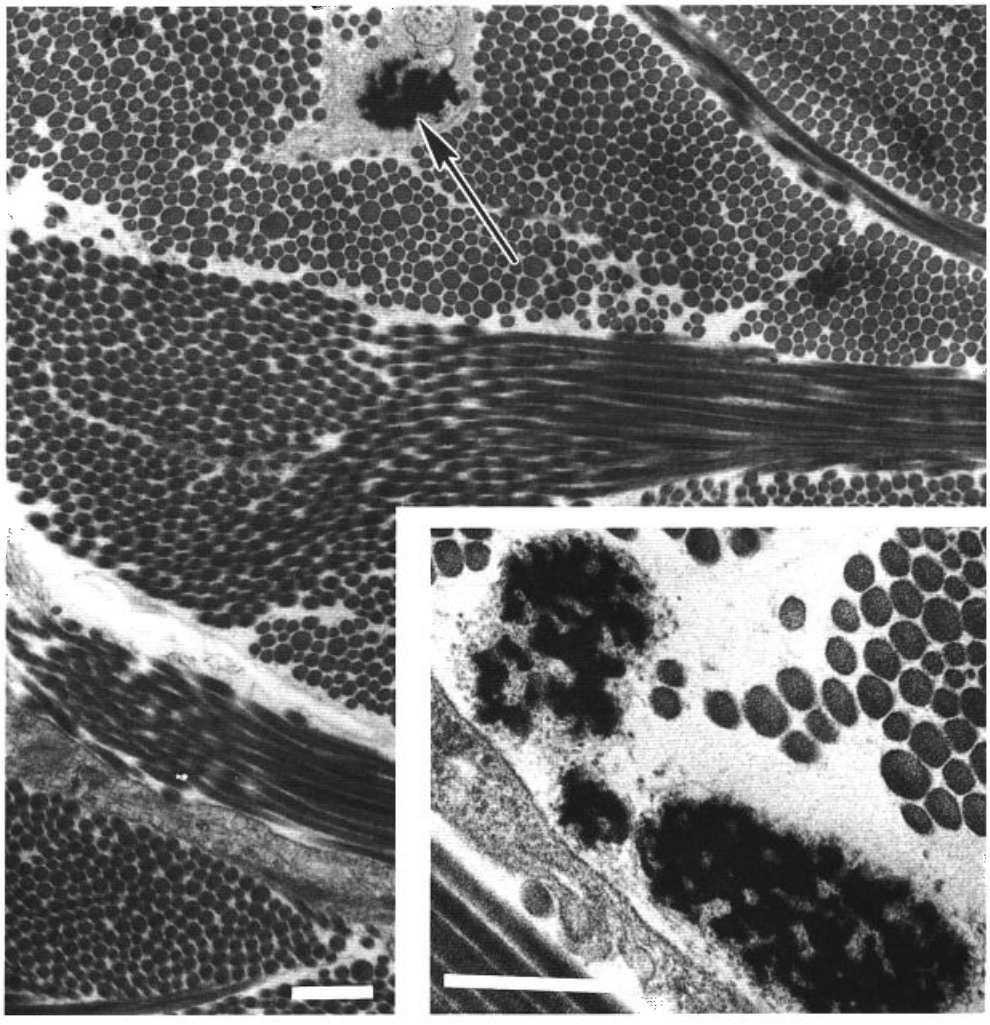

Figure 6. B. SS-A protection prevented elastic fiber hyperplasia and the overproduction of microfibrils. Arrow indicates a small elastic fiber. Magnification ×20,800. Bar = .05 μm. Inset: Typical normal-appearing elastic fibers with black elastin matrix covering most of the microfibrils. Magnification ×44,000. Bar = .05 μm.

DISCUSSION

It was not surprising that avobenzone proved to be highly protective against the damaging effects of chronic UVA I radiation. On the basis of the absorption spectrum, with high absorbance between 310 and 370 nm (8), and its performance in acute-exposure studies (8,13), it was reasonable to expect efficacy. Our results with this particular oxybenzone-containing sunscreen (SS-B) were very surprising. The exacerbation of photodamage, compared to UVA alone, was in total disagreement with our other concurrent findings. Two different oxybenzone-containing sunscreens were tested in parallel with this study, using the same UVA source and irradiation protocol. On the basis of histochemical staining, protection was equal to that of the avobenzone-containing sun-

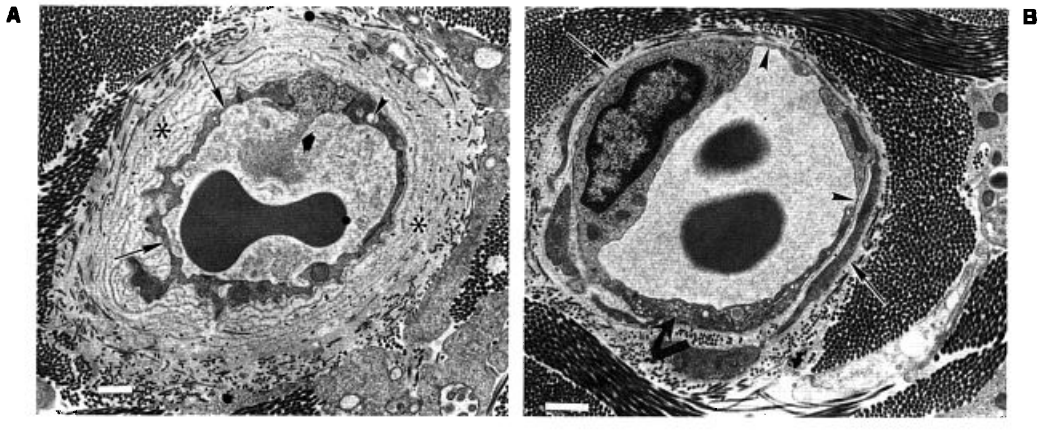

Figure 7. Vasculature. A. UVA radiation-induced extensive basement membrane duplication (*). Endothelial cells were damaged with, among other changes, extensive thinning (→), rupture, retraction or gaps allowing leakage (◗), and swollen mitochanodria (▶). Magnification ×8,300. Bar = 1 μm. B. SS-A prevented vascular damage. The basement membrane (→) was not duplicated. Occasional thin areas (▶) and mild vesiculation (↻) were in the normal range. Magnification ×9,700. Bar = 1 μm.

screen (SS-A), with one exception: SS-A was slightly more effective in preventing the increase in dermal GAGs. Furthermore, these two oxybenzone-containing sunscreens produced no clinical signs of irritation. The absorption spectrum of oxybenzone, with its peak at ~320 nm (8), would not predict such high efficacy against UVA I. However, formulation can be a positive factor. Included in the parallel experiment were findings from other irritating oxybenzone-containing sunscreens. We describe these in reference 14 as a UVA-induced phenomenon that we have termed "photoirritation." From all these results, we conclude that oxybenzone was not the cause of the photodamage observed in this study, but rather some unknown component in the vehicle.

Given our experience with non-irritating oxybenzone-containing sunscreens, it was also surprising that Bissett *et al.* (3) reported that an SPF-15 oxybenzone-containing sunscreen afforded no protection against a total of only 710 J/cm^2 of low-irradiance, long-wavelength UVA as emitted by black-light fluorescent tubes. In our experiments (14) with SPF-15 sunscreens with the same concentration of oxybenzone (3%) as Bissett *et al.* (3) and 8,000 J/cm^2 of high irradiance, long-wavelength UVA, we saw very marked protection. The reasons for such a large discrepancy between our work and that of Bissett *et al.* (3) are not obvious.

The addition of UVA absorbers to UVB absorbers to achieve an SPF of 15 is believed by some to provide adequate protection against UVA since it blocks ~50% of the erythema-effective UVA (15). Furthermore, because it requires 500–1000 times more UVA than UVB to produce erythema in humans (16,17), the probability of accumulating enough UVA to affect connective tissue was thought to be negligible. However, in a recent study to determine an action spectrum for elastosis, Kligman and Sayre (18) found that the amount of UVA I, as delivered by a filtered solar simulator that was required to produce a 50% increase in elastic fiber hyperplasia, was only 30 times greater than for full solar-simulating radiation with its large, highly energetic UVB component. Thus, the histologic consequences of cumulative exposures may require lower multiples of energy compared to those for erythema. If extrapolation from mice to humans, with

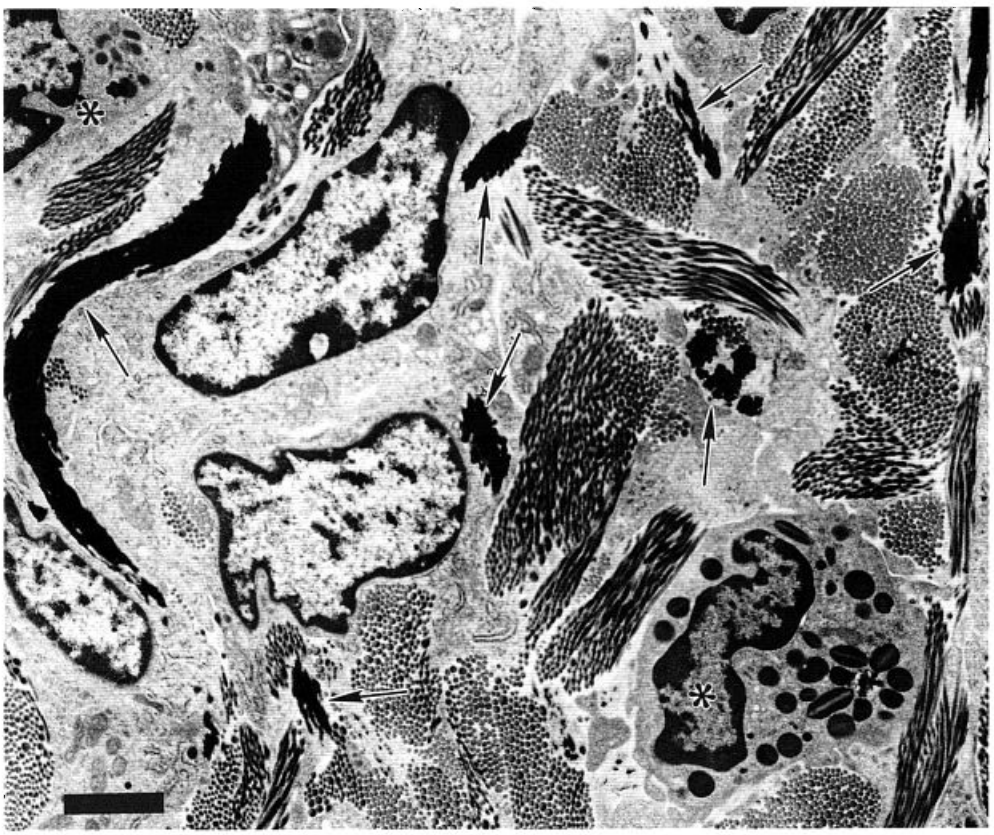

Figure 8. SS-B treated. Elastic fiber (→) hyperplasia was even greater than with UVA alone. Many cells of the inflammatory repertoire were present and eosinophils (*) were abundant. Magnification ×7,800. Bar = 2 μm.

regard to chronic effects of UV radiation, is as valid as a large body of evidence suggests (19), molecules that absorb further into UVA I may be beneficial.

Aside from physical blockers of UV radiation such as thick layers of zinc oxide, all sunscreens allow small amounts of radiation to reach the skin. Whereas erythema can be completely prevented, the cumulative "breakthrough" radiation may contribute to photoaging. We have shown that ½ of a UVA-I MED added to either ¼ or ½ of a UVB MED produces dermal photodamage to hairless mice that is additive (20). Over a lifetime, these small amounts of UVA can add up to thousands of Joules of exposure with detrimental photoaging effects. The argument that SPF-15 sunscreens provide adequate protection against erythema for most people and under most conditions is valid, but acute effects are not the only reason for requiring a sunscreen. Emphasis on acute effects fails to take into consideration the consequences of chronic exposure over a lifetime.

ACKNOWLEDGMENTS

The authors wish to acknowledge the invaluable participation of several associates: Marilyn J. Crosby and Sally Adams, animal treatment; Kermit Wharton, animal care;

Dorothy Campbell, histology procedures; William Witmer, photography; Sijie Zheng, electron micrograph printing; and Brenda Lacey, manuscript preparation.

REFERENCES

(1) L. H. Kligman, F. J. Aiken, and A. M. Kligman, The contributions of UVA and UVB to connective tissue damage in hairless mice, *J. Invest. Dermatol.*, **84**, 272–276 (1983).

(2) L. H. Kligman, K. H. Kaidbey, V. M. Hitchins, and S. A. Miller, Long Wavelength (>340 nm) Ultraviolet-A Induced Skin Damage in Hairless Mice Is Dose Dependent," in *Human Exposure to Ultraviolet Radiation: Risks and Regulations*, W. F. Passchier and B. F. M. Bosnjakovic, Eds. (Elsevier, Amsterdam, 1987), pp. 77–81.

(3) D. L. Bissett, D. P. Hannon, and T. V. Orr, An animal model of solar-aged skin: Histological, physical, and visible changes in UV-irradiated hairless mouse skin. *Photochem. Photobiol.*, **46**, 367–376 (1987).

(4) L. H. Kligman, R. M. Sayre, and K. H. Kaidbey, Dermal damage by short to long wavelengths within the UVA spectrum, *Photochem. Photobiol.*, **45**, 77s (1987).

(5) A. Fourtanier, J. Labat-Robert, and P. Kern, "Effects of Chronic Suberythemal Doses of Pure UVA Radiations—Protective Effect of a New Sunscreen Mexoryl® SX," in *Biologic Responses to UVA Radiation*, F. Urbach, Ed. (Valdenmar Publ. Co., Overland Park, KS, 1992), pp. 393–407.

(6) P. S. Zheng and L. H. Kligman, UVA induced ultrastructural changes in hairless mouse skin: A comparison to UVB-induced damage, *J. Invest. Dermatol.*, **100**, 194–199 (1993).

(7) L. H. Kligman and M. Gebre, Biochemical changes in hairless mouse skin collagen after chronic exposure to UVA radiation, *Photochem. Photobiol.*, **54**, 233–237 (1991).

(8) K. H. Kaidbey and R. W. Gange, Comparison of methods for assessing photoprotection against ultraviolet A in vivo, *J. Am. Acad. Dermatol.* **16**, 346–353 (1987).

(9) J. A. Harrison, S. L. Walker, S. R. Plastow, M. D. Batt, J. L. M. Hawk, and A. R. Young, Sunscreens with low sun protection factor inhibit ultraviolet B and A photoaging in the skin of the hairless albino mouse. *Photoimmunol. Photomed.* **8**, 12–20 (1991).

(10) L. H. Kligman, Luna's technique: A beautiful stain for elastin, *Am. J. Dermatopath.* **3**, 199–200 (1981).

(11) R. Hirose and L. H. Kligman, An ultrastructural study of ultra-violet-induced elastic fiber damage in hairless mouse skin, *J. Invest. Dermatol.*, **90**, 697–702 (1988).

(12) L. H. Kligman, F. J. Akin, and A. M. Kligman, Prevention of ultraviolet damage to the dermis of hairless mice by sunscreens, *J. Invest. Dermatol.*, **78**, 181–189 (1982).

(13) J. R. Lowe, M. M. Mobayen, T. Bourget, and S. H. Dromgoole, UVA protection in human epidermis: Comparison of three sunscreen formulations, *J. Invest. Dermatol.*, **94**, 551 (1990).

(14) L. H. Kligman, Photoirritation in hairless mice: A novel UVA-dependent phenomenon, *Photochem. Photobiol.*, **53**, 127s (1991).

(15) C. A. Cole and R. Van Fossen, "Testing UVA Protective Agents in Man," in *Biologic Responses to UVA*, F. Urbach, Ed. (Valdenmar Publ. Co., Overland Park, KS, 1992), pp. 335–345.

(16) K. H. Kaidbey and A. M. Kligman, The acute effects of long-wave ultraviolet radiation on human skin, *J. Invest. Dermatol.*, **72**, 253–256 (1979).

(17) C. Y. Ying, J. A. Parrish, and M. A. Pathak, Additive erythemogenic effects of middle (280–320 nm) and long-wave (320–400 nm) ultraviolet light, *J. Invest. Dermatol.*, **63**, 273–278 (1974).

(18) L. H. Kligman and R. M. Sayre, An action spectrum for ultraviolet induced elastosis in hairless mice: Quantification of elastosis by image analysis. *Photochem. Photobiol.* **53**, 237–242 (1991).

(19) L. H. Kligman, The hairless mouse and photoaging. Yearly Review. *Photochem. Photobiol.*, **54**, 1109–1118 (1991).

(20) L. H. Kligman, UVA enhances low dose UVB tumorigenesis, *Photochem. Photobiol.*, **47**, 8s (1988).